American Journal of Pathology, Vol. 165, No. 3, September 2004

Animal Model

Cerebellar Ataxia, Seizures, Premature Death, and Cardiac Abnormalities in Mice with Targeted Disruption of the *Cacna2d2* Gene

Sergey V. Ivanov,*† Jerrold M. Ward,‡ Lino Tessarollo,§ Dorothea McAreavey,¶ Vandana Sachdev,‖ Lameh Fananapazir,‖ Melissa K. Banks,** Nicole Morris,†† Draginja Djurickovic,†† Deborah E. Devor-Henneman,‡ Ming-Hui Wei,† Gregory W. Alvord,‡‡ Boning Gao,§§ James A. Richardson,¶¶ John D. Minna,§§ Michael A. Rogawski,** and Michael I. Lerman†

From the Basic Research Program, the Laboratory Animal Sciences Program,†† Science Applications International Corporation-Frederick, Inc., National Cancer Institute at Frederick, Frederick, Maryland; the Laboratory of Immunobiology,† Veterinary and Tumor Pathology Section,‡ the Mouse Cancer Genetics Program,§ Neural Development Section, Computer and Statistical Services,‡‡ Center for Cancer Research, National Cancer Institute at Frederick, Frederick, Maryland; the Clinical Center,¶ Clinical Electrophysiology and Inherited Heart Diseases Section,‖ Cardiology Branch, National Heart, Lung, and Blood Institute, Epilepsy Research Section,** Division of Intramural Research, National Institute of Neurological Disorders and Stroke, National Institutes of Health, Bethesda, Maryland; and the Hamon Center for Therapeutic Oncology Research§§ and the Department of Pathology,¶¶ University of Texas, Southwestern Medical Center, Dallas, Texas*

CACNA2D2* is a putative tumor suppressor gene located in the human chromosome 3p21.3 region that shows frequent allelic imbalances in lung, breast, and other cancers. The α2δ-2 protein encoded by the gene is a regulatory subunit of voltage-dependent calcium channels and is expressed in brain, heart, and other tissues. Here we report that mice homozygous for targeted disruption of the *Cacna2d2* gene exhibit growth retardation, reduced life span, ataxic gait with apoptosis of cerebellar granule cells followed by Purkinje cell depletion, enhanced susceptibility to seizures, and cardiac abnormalities. The *Cacna2d2*^{tm1NCIF} null phenotype has much in common with that of *Cacna1a* mutants, such as cerebellar neuro-degeneration associated with ataxia, seizures, and premature death. A tendency to bradycardia and limited response of null mutants to isoflurane implicate α2δ-2 in sympathetic regulation of cardiac function. In summary, our findings provide genetic evidence that the α2δ-2 subunit serves *in vivo* as a component of P/Q-type calcium channels, is indispensable for the central nervous system function, and may be involved in hereditary cerebellar ataxias and epileptic disorders in humans. *(Am J Pathol 2004, 165:1007–1018)

Voltage-dependent calcium channels (VDCCs)[1] play a role in generating the rhythmic membrane potential behavior of many excitable cells and also provide a pathway through which Ca^{2+} enters cells to serve as a second messenger that regulates a diversity of cellular processes.[1–3] VDCCs consist minimally of an α1 protein that forms the channel pore and voltage-sensor. Core α1 subunits are used for dividing VDCCs into three major phylogenetic types, which are supported by pharmacological and functional classification: T-type ($\alpha1_G$, $\alpha1_H$, and $\alpha1_I$); L-type ($\alpha1_C$, $\alpha1_D$, $\alpha1_F$, and $\alpha1_S$); and the presynaptic channels-type ($\alpha1_A$, $\alpha1_B$, and $\alpha1_E$).[4] A variety of auxiliary regulatory subunits, including α2δ, β, and γ, associate with the α1-subunits, forming different heteromeric functional VDCCs.[5–7] The members of the α2δ family include α2δ-1, which is ubiquitously expressed; α2δ-2, which is expressed in brain, heart, and other organs; and α2δ-3, whose transcripts are found mostly in the brain.[8–10] α2δ subunits consist of two proteins that are encoded by a single gene, the product of which is post-translationally cleaved from a single polypeptide precursor.[10,11] The discovery of worm and fly orthologs of α2δ-encoding genes[12] demonstrates their conservation

Supported in part with federal funds from the National Cancer Institute, National Institutes of Health, under Contract No. NO1-CO-12400.

Accepted for publication May 17, 2004.

Address reprint requests to Sergey V. Ivanov, Building 560, NCI-Frederick, P.O. Box B, Frederick, MD 21702-1201. E-mail: ivanov@mail.ncifcrf.gov.

over billions of years of evolution, suggesting that the $\alpha 2\delta$ protein is of fundamental importance in cellular function.

In humans, $\alpha 2\delta$-2 is encoded by *CACNA2D2* (GenBank Accession No. AF040709), which is contained, along with seven other genes, in a 120-kb region of chromosome 3p21.3 that is frequently deleted in lung, breast, and other cancers.[12] Reduction or absence of *CACNA2D2* expression in non-small cell lung cancer cell lines suggests that $\alpha 2\delta$-2 itself may be a tumor suppressor protein. $\alpha 2\delta$-2 is predicted to be a heavily glycosylated 175-kd protein whose single-pass transmembrane δ piece anchors the $\alpha 2$ protein to the membrane.[13]

Electrophysiological studies demonstrated that $\alpha 2\delta$-2 might function as an auxiliary component of a variety of different VDCCs: L-type [$Ca_v1.2$ (α_{1C})]; P/Q-type [$Ca_v2.1$ (α_{1A})]; N-type [$Ca_v2.2$ (α_{1B})]; R-type [$Ca_v2.3$ (α_{1E})]; and T-type [$Ca_v3.1$ (α_{1G}) and $Ca_v3.2$ (α_{1H})].[8,9,14] Co-expression of $\alpha 2\delta$-2 with each of these α_1 subunits enhanced currents through the heteromeric channels. While these experiments characterized $\alpha 2\delta$-2 as electrophysiologically versatile, its biological significance remained uncertain. Here we report that the *Cacna2d2* null mice show ataxia, growth retardation, increased susceptibility to seizures, and a reduced life span. Phenotypic similarity with *Cacna1a* null mice and spontaneous *Cacna1a* mutants implicates $\alpha 2\delta$-2 in regulation of P/Q-type currents as a component of Cav2.1 channels and suggests a possible involvement of the gene in human hereditary cerebellar ataxias and epilepsies. We also provide evidence that $\alpha 2\delta$-2 expression in the central nervous system, dorsal sympathetic ganglia, and cardiac conductive tissue may be related to the observed disturbances in null mutants' heart rate regulation.

Materials and Methods

Construction of Targeting Vector and Generation of *Cacna2d2*^{tm1NCIF} Mice

A replacement-type *Cacna2d2*-targeting vector was based on a mouse genomic clone isolated from a 129/SvJ lambda FIXII library (Stratagene, La Jolla, California). *Cacna2d2* exons were identified by Southern hybridization, partial sequencing, and BLAST analysis. Mouse EST clone represented in GenBank by Accession No. AA000341 (Research Genetics, Huntsville, AL) was used as a probe. A 2629-bp fragment containing eight exonic fragments (positions 2517 to 3184 in the mouse *Cacna2d2* mRNA AF247139) and a 6.3-kb fragment representing the 3′ non-coding region of *Cacna2d2* were integrated into the construct as 5′ and 3′ flanking sequences, respectively. The neo-gene with the phosphorglycerol kinase 1 promoter and the bovine growth hormone polyadenylation sequence (pGKneobpA) was used as a positive selectable marker; the pGK-thymidine kinase cassette was used as a negative selectable marker.[15] Electroporation and selection were performed using CJ7 ES cell line, as described elsewhere.[16] DNAs derived from G418/FIAU-resistant ES clones were screened using a diagnostic *Eco*RI restriction enzyme sites and the 2.0-kb 3′ probe external to the targeting sequence indicated in Figure 1A. This probe detects a ~20-kb *Eco*RI fragment in wild-type DNA and an 8.3-kb *Eco*RI-fragment in a mutant allele. Two independent *Cacna2d2*-targeted cell lines were isolated and one of those, when injected into C57BL/6J blastocysts, transmitted the mutant allele to the offspring generating chimeras. Chimeras were then identified by the agouti coat color. Male chimeras were mated with C57BL/6J females and agouti-colored offspring were genotyped by tail clip. Chimeras that transmitted the *Cacna2d2*^{tm1NCIF} allele through the germline were then mated to C57BL/6J females to establish lines.

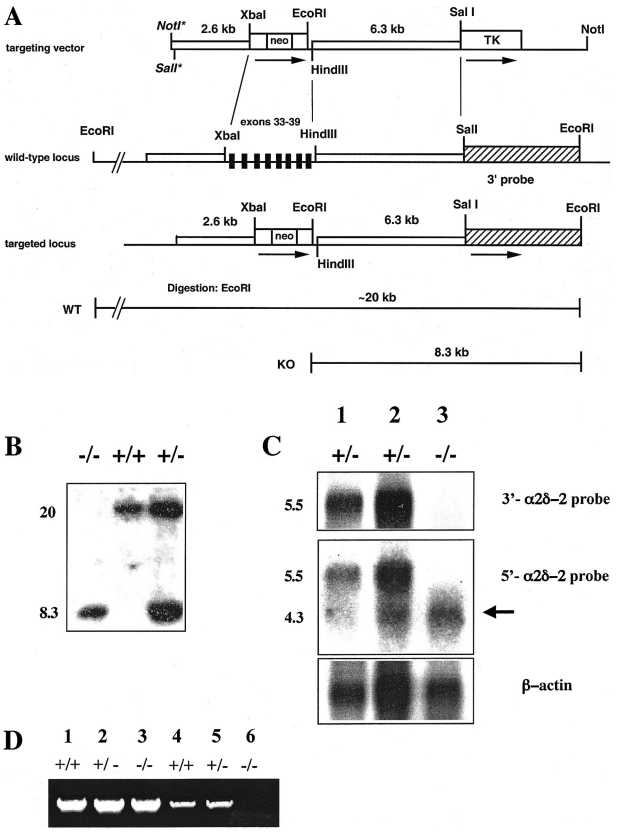

Figure 1. Targeted disruption of *Cacna2d2*. **A:** Strategy for targeted disruption of *Canca2d2*. Seven 3′-terminal exons of *Cacna2d2* replaced by homologous recombination with a neomycin-resistance gene are shown by **vertical bars**. The recombination caused a decrease in size of the *Eco*RI restriction fragment, which was revealed by Southern blot analysis with the *SalI*/*Eco*RI fragment (**hatched box**). Restriction sites introduced from the phage lambda cloning site are marked with asterisks. **B:** Southern blot analysis of wild-type (+/+) and targeted (+/−, −/−) mice. The 8.3-kb *Eco*RI-band serves as a marker for the targeted *C* 127 *a* 127 *c* 127 *n* 127 *a* 127 *2* 127 *d* 127 *2*^{tm1NCIF} allele. **C:** Northern analysis of *Cacna2d2* expression in brains from *Cacna2d2*-targeted mice: truncated *Cacna2d2* mRNA in null-mutants that encodes an aberrant protein devoid of membrane-binding capacity could be detected with a 5′ probe (positions 1742–2862, GenBank Accession No. AF247139), but not with a 3′ cDNA probe that represents the substituted C-terminal part of the $\alpha 2\delta$-2 protein (positions 3237–5498). **Lane 2** contains twice the amount of RNA to reveal the truncated transcript. **D:** RT-PCR on total RNA isolated from brain confirms the absence of the targeted 3′ portion of the *Cacna2d2* transcript. **Lanes 1–3:** RT-PCR products generated with a primer set representing positions 1742–2862; **Lanes 4–6:** RT-PCR products obtained with primers representing positions 3113–4149, GenBank Accession No. AF247139.

mRNA Expression Analysis

RT-PCR on mouse RNA samples was performed using a SuperScript One-Step RT-PCR kit (Invitrogen, Carlsbad,

CA) according to the manufacturer's protocol. Two primer sets were used for RT-PCR. One of them, 5′-GCATAACTATGATGTCACAC-3′ and 5′-GGGGCTT-GAAGATATAACCA-3′, represented a *Cacna2d2* cDNA fragment with positions 1742–2862. The other pair, 5′-TCTACTCTGTGTCCTCATTG-3′ and 5′-TGAGTCTAGG-GACTGTGGG-3′, corresponded to positions 3113–4149 (GenBank Accession No. AF247139). Comparative PCR on human cardiovascular MTN cDNA panel (Clontech, Palo Alto, CA) was performed as suggested by the manufacturer with human primers 5′-GCATAACTATGACGT-CACAC-3′ and 5′-GGGGCTTGAAGACATAACCG-3′ corresponding to the first set of mouse primers. Northern analysis and RT-PCR were performed on mouse brain mRNAs isolated with a FastTrack 2.0 kit (Invitrogen). A *Cacna2d2* cDNA EST clone (GenBank Accession No. AA000341, positions 3237–5498 in AF042792) purchased from Genome Systems, Inc. (St. Louis, MO) was used as a 3′ probe, while the RT-PCR product obtained with the first set of primers (see above) was used as a 5′ probe. The same mouse EST clone was also used to generate ^{35}S-labeled RNA probes for *in situ* hybridization on mouse tissues. These probes were synthesized using MAXIscript (Ambion Inc., Austin, TX) *in vitro* transcription kit and two primers. Primer 5′TAATACGACTCACTAT-AGGGAGAcctatgactatcaggcag-3′ contained T7 RNA-polymerase promoter shown in uppercase and was used to produce sense probe. Primer 5′AATTAACCCTCACTA-AAGGGAGAccacagtctgaggtatct-3′ contained T3 RNA-polymerase promoter and was used to generate antisense probe. DNA template used in the RNA synthesis was eliminated with DNase I following the *in vitro* transcription reaction. For *in situ* hybridization, tissues of postnatal mice or embryos at stages 13.5 and 15 dpc were perfused and fixed as described.[17] Briefly, the samples were hydrated, paraffin-embedded, and sectioned at 4 mm onto microscope slides. For pre-hybridization, the slides were deparaffinized in xylene, hydrated through a series of graded ethanol/DEPC-saline, put through a microwave RNA retrieval procedure, and the RNA was further unmasked by permeabilization with pronase. For hybridization, a riboprobe 750,000 cpm was added to the hybridization buffer,[17] denatured at 95°C for 5 minutes, and incubated with the slides for 14 hours at 55°C. Slides were washed in the washing buffer, incubated with RNase A, dehydrated in graded ethanol rinses, and dried under vacuum. Dried slides were immersed into twofold-diluted K.5 nuclear emulsion (Polysciences, Warrington, PA), slowly dried at room temperature, and exposed for 14 days. The slides were then developed using D19 reagent (Eastman Kodak, Rochester, NY), and latent images fixed using Kodak Fixer. The slides were finally thoroughly rinsed, counterstained with hematoxylin (Richard-Allen, Kalamazoo, MI), dehydrated, and glass-covered using permanent mounting media. Visualization of signal was done on a Leitz Laborlux-S (Wetzlar, Germany) microscope.

Animal Testing

Animals used in these studies were maintained in facilities fully accredited by the Association for Assessment and Accreditation of Laboratory Animal Care and all procedures were performed under protocols approved by the NIH (Publication No. 86–23, 1985) and NCI Animal Care and Use Committees in strict compliance with the Guide for the Care and Use of Laboratory Animals of the National Research Council (National Academy Press, Washington, DC; http://www.nap.edu/readingroom/books/labrats).

Seizure Susceptibility Testing

Twelve- to 24-week-old mice were used. Pentylenetetrazol (PTZ) (Sigma-Aldrich, St. Louis, MO), in 0.9% NaCl solution, was administered by subcutaneous injection into a loose fold of skin on the right belly. Mice were observed for 30 minutes. Animals exhibiting a clonic spasm of at least 5 seconds duration were scored as positive for seizure occurrence. To determine the 50% convulsive dose (CD_{50}) a range of PTZ doses were used spanning the CD_{50} value. Each mouse received only a single injection and the animal was immediately euthanized after exhibiting convulsions or at the end of the 30-minute observation period. In a separate series of experiments the behavioral seizure score was determined with increasing cumulative doses of PTZ. Mice (18 to 24 weeks old) were injected intraperitoneally with a 10 mg/kg dose of PTZ and observed for 30 minutes. Additional doses of 20, 40, and 60 mg/kg were administered at 30-minute intervals until tonic hind limb extension occurred, at which time the mice were immediately euthanized. PTZ typically induced a sequence of behaviors that were scored in each of the 30-minute intervals after dosing according to the following scale: 0, normal behavior; 1, behavioral arrest; 2, vocalization and limb twitches; 3, sustained fore limb clonus; 4, wild running and jumping; and 5, tonic hind limb extension.

Inverted Screen Test

A modification of the horizontal screen test was used as a measure of overall motor function.[18] Mice were placed on a horizontally oriented grid (consisting of parallel 1.5-mm diameter rods situated 1 cm apart), and the grid was inverted. The time the animal remained on the underside of the grid was recorded. Mice that fell from the grid within $<$15 seconds were considered to have reduced strength or coordination.

Footprint Pattern Test

Mice with hind paws dipped in non-toxic ink were placed at one end of a dark tunnel measuring 10 cm $\times$ 10 cm $\times$ 50 cm, the bottom of which was lined with white paper. Mice walked down the tunnel, and their footprints were used to assess the ability to walk in a straight line, irregularities, and orientation of the hind paws.[19]

Echocardiography

Trans-thoracic echocardiography was performed using an Acuson Sequoia equipped with a 15-MHz linear trans-

ducer (15L8) in a phased-array configuration. Animals were placed on a heating pad (37°C) and imaged under isoflurane anesthesia in the left lateral decubitus position. Two-dimensional images were obtained from parasternal long- and short-axis views with optimized gain and depth settings. M-mode images were obtained from short-axis views at the papillary muscle level at a sweep speed of 100 mm/s. Two-dimensional and M-mode images were digitized and stored for off-line analysis. Cardiac measurements were performed off-line from the M-mode images using a leading edge-to-leading edge technique according to the American Society of Echocardiography guidelines.[20] Measurements from five cardiac cycles were averaged to obtain the following parameters in diastole and systole: interventricular septum (IVSd, IVSs); posterior wall (PWd, PWs); and left ventricular internal diameter (LVIDd, LVIDs). The percentage of LV fractional shortening (LV% FS) was calculated as {(LVIDd − LVIDs/LVIDd} × 100. LV mass was calculated according to the uncorrected cube method using the equation LV mass (mg) = 1.055{(IVSd+LVIDd+PWd)^3 − (LVIDd)^3}, as previously reported.[21]

ECG Recordings

ECGs were recorded in conscious and sedated mice with different *Cacna2d2* status using a recently developed noninvasive ECG recording device and software (Mouse Specifics, Boston, MA), as described previously.[22] Conscious or isoflurane-sedated animals were positioned on the ECG platform with gel-coated electrodes embedded in its base. The amplified signals were digitized with 16-bit precision at a sample rate of 2000 samples/second. Only continuous recordings (>10 to 25 ECG complexes) generated from mice with three paws in contact with three electrodes were analyzed. The following parameters were measured: HR and RR interval, PR interval, QRS duration and maximum height, QT and corrected QT intervals.

Blood Pressure Measurements and Clinical Chemistry

Noninvasive blood pressure and serum electrolytes were measured on each of four null and five wild-type animals by Phenotyping Service of the Jackson Laboratory (West Sacramento, CA). Growth hormone, T3, T4, and IGF-1 serum levels in each of four null and four wild-type animals were assayed by Anilytics, Inc. (Gaithersburg, MD).

Pathology

Cacna2d2$^{+/+}$, *Cacna2d2*$^{+/-}$, and *Cacna2d2*$^{-/-}$ male and female mice from 22 days to 70 days of age were completely necropsied. All tissues were fixed in neutral buffered formalin, embedded in paraffin, sections cut at 4 to 6 μm, and stained with hematoxylin and eosin (H&E). Selected tissues were stained with luxol fast blue and Bodian stains. For immunohistochemistry of the brain, antibodies to glial fibrillary acidic protein (GFAP) (DAKO, Carpinteria, CA), Ki-67 (polyclonal, Novocastra, Newcastle on Tyne, UK), calbindin (D-28K, Sigma), and caspase-3 (Promega, Madison, WI) were used. The TUNEL method (ApopTag® *In Situ* Apoptosis Detection kit, Intergen, Purchase, NY) was used to identify apoptotic cells.

Statistics

Data in this study were evaluated using standard analysis of variance and Student's *t*-tests, repeated measures analysis of variance, profile analysis, analysis of covariance, post-hoc tests, non-parametric methods, survival analysis, and graphical descriptive techniques. Data analyzed with parametric methods were routinely tested for conformance with homogeneity of variance and covariance requirements. Kaplan-Meier plots were constructed for survival, and differences in survival distributions were tested with the log rank test.

Results

Generation and Characterization of Cacna2d2^{tm1NCIF} Mice

We constructed a *Cacna2d2*-targeting vector, in which a 3445-bp *Xba*I/*Hind*III fragment (positions 6593434–6596878 on NT_039477) containing seven 3′-terminal exons of the gene was replaced by a neomycin-resistance gene (Figure 1A). This replacement eliminated the sequence encoding the entire δ subunit with a single transmembrane domain plus the 87 C-terminal amino acids of the α2 responsible for binding the δ subunit. Genotyping of 256 F_2 offspring by Southern hybridization (Figure 1B) revealed a *Cacna2d2*$^{+/+}$: *Cacna2d2*$^{+/-}$: *Cacna2d2*$^{-/-}$ distribution (64:130:62) that was very close to the expected Mendelian distribution. Northern blot analysis on brain mRNAs showed expression of the full-length transcript in heterozygotes but not null-mutant animals (Figure 1, C and D).

Growth Delay, Neurological Phenotype, and Premature Death in Null-Mutants

While *Cacna2d2*$^{+/-}$ mice appeared healthy, had normal life spans, and were not distinguishable from their *Cacna2d2*$^{+/+}$ littermates in any assay, null-mutants could be reliably identified at approximately 4 weeks of age and older by dystonic episodes, ataxic waddling gait typical for cerebellar dysfunction, and reflexive clutching of hind limbs when lifted by their tails (Figure 2). Dystonic episodes usually started with characteristic extension of the hind limbs. During the next stage that lasted from a few minutes to more than one-hour, conscious animals were immobilized on their abdomen or side by whole-body extension. After recovery, the null-mutants walked in a poorly coordinated fashion, dragging their hind limbs and often listing to one side. They frequently showed myo-

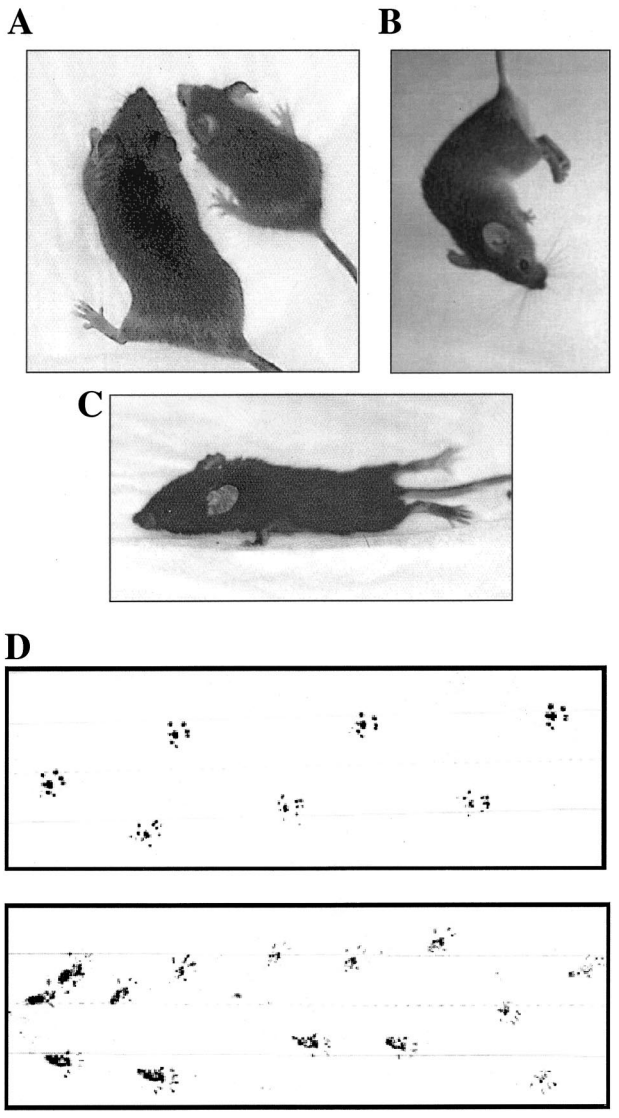

Figure 2. Canca2d2-null mice show growth retardation and motor impairment. **A:** Wild-type mouse (**left**) next to its *Cacna2d2*$^{-/-}$ sibling. **B:** When held vertically by tail, null mutants show hind limb clasping, a common hallmark of neuropathology. **C:** Spontaneous tonic hind limb extension. **D:** Null-mutants (**bottom lane**) show irregularly spaced, outwardly oriented footprints ("ducky" gait) as compared to the wild-type footprints (**upper lane**).

clonic jerking of the limbs or whole body tremor, and tonic extension of the hind limbs. In four animals, generalized clonic seizures that lasted up to 30 minutes and affected the entire body were observed. The null-mutants developed growth delay starting at the age of 4 weeks ($P <$ 0.0001 by analysis of covariance, profile analysis, and post-hoc *t*-tests). The mean body weights of *Cacna2d2*$^{-/-}$ mice were ~1.5 to 2 times less than that of their wild-type age mates (Figure 3A). *Cacna2d2*$^{-/-}$ mice also had markedly reduced life spans ($P < 0.0001$ by the log rank test), with a median survival time of 150 days (Figure 3B). Among 50 *Cacna2d2*$^{-/-}$ mice studied, 23 (46%) died prematurely with no obvious cause of death. Most of these mice died at young ages, and no premature deaths were observed at ages older than 6 months (Figure 3B).

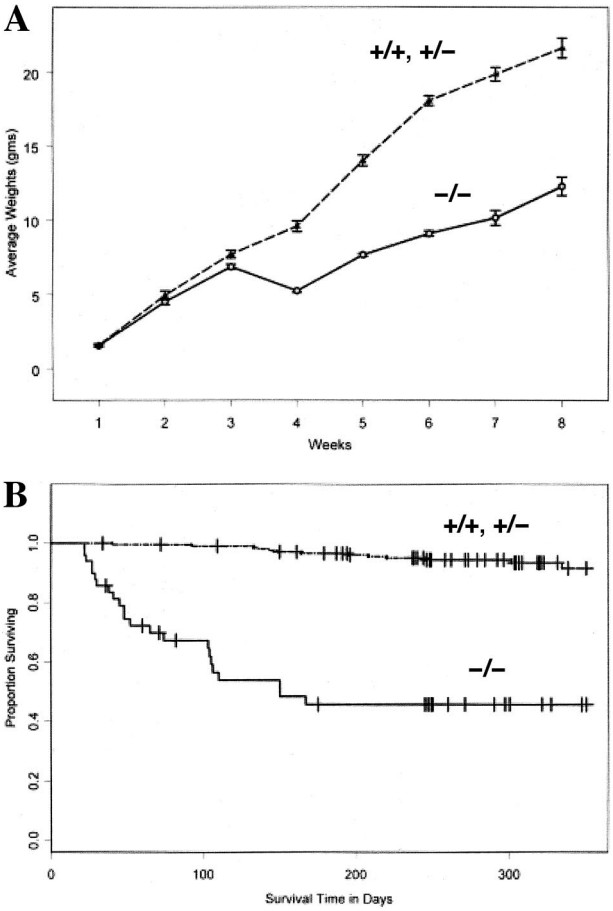

Figure 3. Growth delay and premature death in *Cacna2d2*$^{-/-}$ mice. **A:** Differences in body weights between *Cacna2d2*$^{-/-}$ ($n = 7$ for weeks 1 to 4; $n = 4$ for weeks 5 to 8) and control mice ($n = 12$) are highly significant ($P <$ 0.0001) from week 4 on. **B:** Kaplan-Meier curves showing highly significant ($P < 0.0001$) survival differences between *Cacna2d2*$^{-/-}$ ($n = 50$) and control mice ($n = 214$). Censored observations (life spans of sacrificed animals) are shown with **vertical bars**.

Evaluation of Motor Function

Motor impairment in null-mutants was evaluated with the inverted screen test, in which the animals were required to support their body weight by grasping a wire grid. None of 6 *Cacna2d2*$^{-/-}$ remained on the inverted screen for at least 15 seconds, whereas 3 of 6 of the *Cacna2d2*$^{+/-}$ and 6 of 7 of the *Cacna2d2*$^{+/+}$ remained on the grid. The mean times on the grid were 5.5 ± 1.5 seconds, 56 ± 23 seconds, and 138 ± 83 seconds, respectively. Compared with wild-type control mice, *Cacna2d2*$^{-/-}$ mice had significant motor impairment ($P = 0.006$, Kolmogorov-Smirnov test). Heterozygotes were not significantly different ($P = 0.713$) from wild-type mice.

Cacna2d2 Expression in Mouse Tissues

In situ hybridization with mouse embryo and adult cerebellum sections showed that *Cacna2d2* is expressed primarily in the central nervous system (Figure 4). In the postnatal cerebellum, a very high level of gene expression was detected in the Purkinje cell layer, while granular

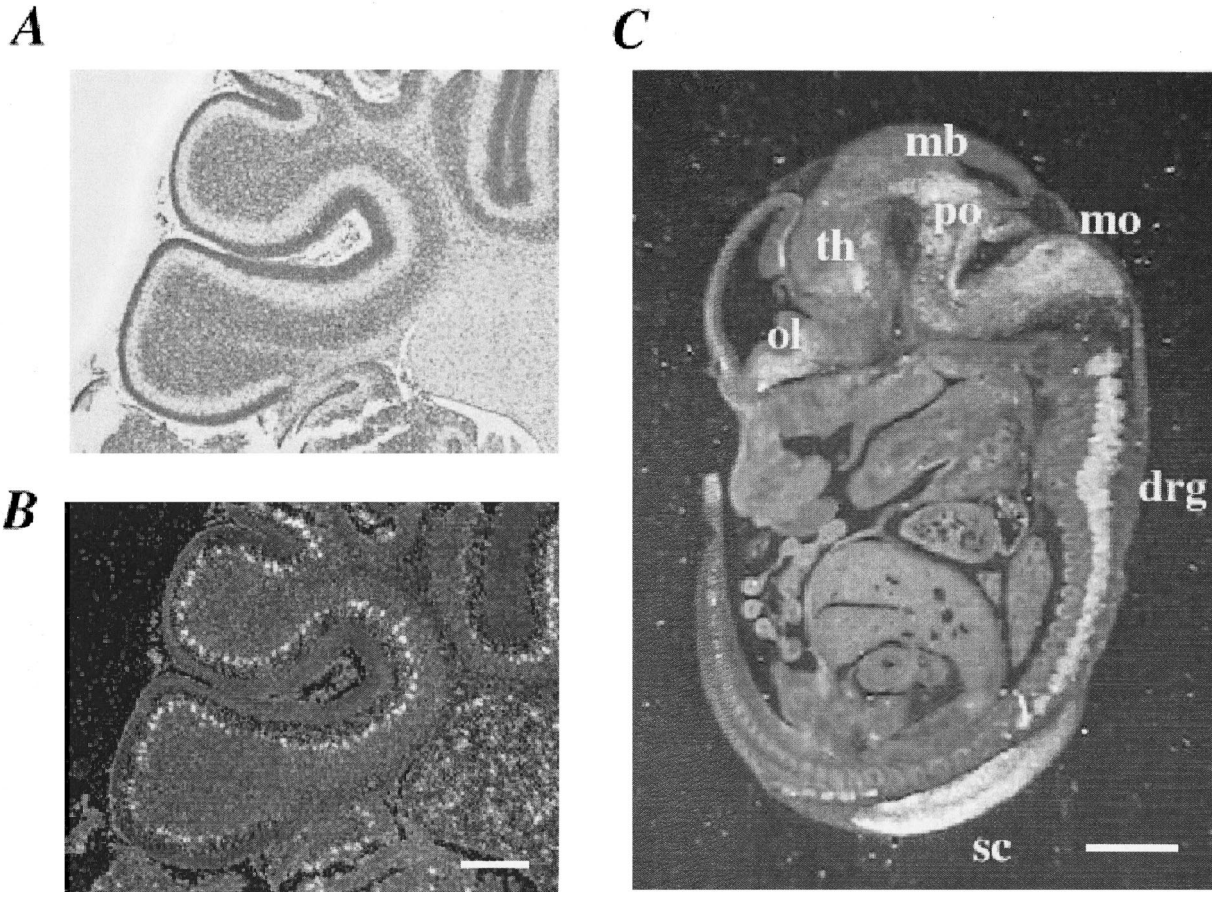

Figure 4. *Cacna2d2* expression in mouse postnatal cerebellum and embryo. Sagittal section of a P15 normal cerebellum in a bright field (**A**) and in a dark field (**B**) after *in situ* hybridization with a *Cacna2d2* probe (**white bar** corresponds to 0.2 mm). *In situ* experiment on a 13.5 dpc embryo (**C**) shows that *Cacna2d2* is highly expressed in CNS and sympathetic spinal ganglia (**white bar** corresponds to 1 mm). Major areas of gene expression are: ol, olfactory lobe; th, thalamus; mb, midbrain; po, pons; mo, medulla oblongata; drg, dorsal ganglia; sc, spinal cord.

produced poor signals (Figure 4, A and B). Remarkably, *Cacna2d2* expression was also detected outside the central nervous system, namely, in the dorsal sympathetic ganglia (Figure 4C). While no *Cacna2d2* expression was detected in mouse embryonic heart, previous reports indicated that this gene is highly expressed in both mouse and human adult hearts.[8–10] Indeed, using the RT-PCR assay we demonstrated that the *CACNA2D2* mRNA is expressed mainly in four cardiac regions: auricles, aorta, interventricular septum, and atrioventricular node (Figure 5). These areas represent highly innervated parts of the heart's conductive system. Limited levels of *CACNA2D2* expression were also detected in the muscle tissue, such as apex and ventricles.

Assessment of Cardiac Function

To explore the possibility of heart failure due to the $\alpha 2\delta$-2 deficiency we evaluated null mutants' heart function. First, histo-pathological study of the null mutants' hearts revealed no signs of cardiomyopathy, apoptosis, or any other abnormality (data not shown). Second, heart function was assessed *in vivo* by surface electrocardiography (ECG) and *trans*-thoracic echocardiography. A trend to bradycardia was revealed in conscious null-mutants as compared to the *Cacna2d2*$^{+/-}$ and *Cacna2d2*$^{+/+}$ control group (747 ± 53 versus 714 ± 73, control versus knockout, $P = 0.07$, Table 1). No significant differences were observed in other major ECG parameters. Remarkably, isoflurane anesthesia produced different effects on heart rates in two cohorts. While in both cases isoflurane reduced heart rate, the null-mutants' response was less profound than that of the control cohort (186 ± 37 versus 102 ± 44, control versus knockout, $P = 0.01$, Table 1). Consistent with the previous histopathological evaluation, echocardiographic study showed no evidence of systolic abnormalities in the null mutants' echocardiograms, and

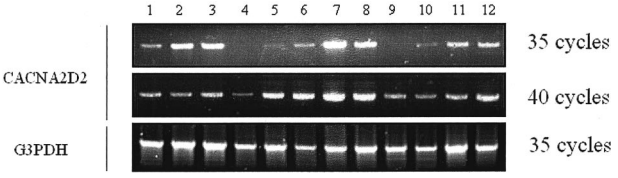

Figure 5. PCR analysis of *CACNA2D2* expression on human heart cDNA panel. **Lane 1**, adult heart; **lane 2**, fetal heart; **lane 3**, aorta; **lane 4**, apex of the heart; **lane 5**, atrium, left; **lane 6**, atrium, right; **lane 7**, auricle, dextra; **lane 8**, auricle, sinistra; **lane 9**, ventricle, left; **lane 10**, ventricle, right; **lane 11**, interventricular septum; **lane 12**, atrioventricular node. The 35-cycle PCR shows significant differences between heart areas in the *CACNA2D2* mRNA content. G3PDH transcripts are used as a control.

Table 1. Major ECG Parameters in Wild-Type and *Cacna2d2*$^{-/-}$ Mice

Parameter	Control	Null	*p*-value
Heart rate (bpm)	747 (53)	714 (73)	MS (0.07)
RR interval (ms)	81 (7)	86 (10)	MS (0.07)
PR interval (ms)	27 (3)	26 (3)	NS
QRS duration (ms)	11 (1)	11 (1)	NS
QT interval (ms)	42 (5)	43 (4)	NS
QTc interval (ms)	46 (3)	46 (2)	NS
ΔHR_{iso}	186 (37)	102 (44)	0.01
ΔRR_{iso}	27 (9)	14 (7)	0.04

Mean (standard deviation); *p*-values computed with Student's *t* test; QTc, corrected QT interval; for baseline measurements, 29 null-mutants and 29 control animals were studied; for isoflurane study, 6 null and 6 control mice were analyzed; NS, not significant; MS, marginally significant; ΔHR_{iso}, decrease in heart rate in response to isoflurane; ΔRR_{iso}, increase in RR interval in response to isoflurane.

no significant differences in IVSd, IVSs, PWd, PWs, LVIDd, LVIDs, LV%FS, and LV mass were found between null mutants and wild-type animals (6 null-mutants and 6 wild-type animals; data not shown). No significant differences were detected in blood pressure and serum electrolyte concentrations between *Cacna2d2*$^{-/-}$ mice and a control group (potassium, sodium, magnesium, and calcium measurements on five wild-type and four homozygous mutant mice; data not shown).

PTZ Seizure Test

As noted, Cacna2d2$^{-/-}$ mice exhibited sporadic behavioral seizures. To further pursue the possibility of an epileptic phenotype, seizure susceptibility was determined with the convulsant PTZ. For all genotypes, there was a dose-dependent increase in the fraction of animals exhibiting clonic seizures with PTZ doses in the range of 10 to 80 mg/kg (Figure 6A). However, the dose-response curve for *Cacna2d2*$^{-/-}$ mice was significantly shifted to the left compared with the curves for *Cacna2d2*$^{+/-}$ and *Cacna2d2*$^{+/+}$ littermates, indicating that the null mutants have greater seizure susceptibility. In a separate series of experiments examining the behavioral seizure score with cumulative dosing of PTZ, all genotypes exhibited a dose-dependent increase in the seizure score with PTZ doses in the range 10 to 60 mg/kg, and all showed tonic hind limb extension at PTZ doses of 60 mg/kg or less. As shown in Figure 6B, null mutant mice exhibited higher seizure scores than their littermates at 10 and 20 mg/kg cumulative doses of PTZ, indicating that they experience more severe seizures at these doses. Both studies indicate that the null mutants have enhanced seizure susceptibility.

Pathology, Histology, and Immunohistochemistry

At necropsy, the null mice were runty as compared to *Cacna2d2*$^{+/+}$ or *Cacna2d2*$^{+/-}$ littermates, dehydrated, and had little fat. Because ataxia is a clinical manifestation of disturbance in coordinated motor activity, which may be caused by cerebellar impairment, we compared

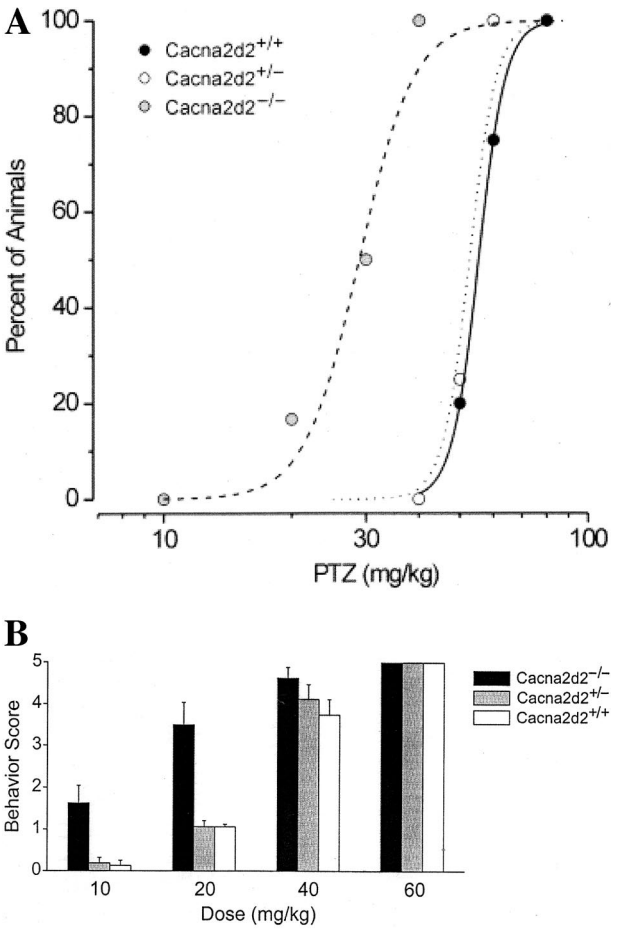

Figure 6. *Cacna2d2* null mice show increased seizure susceptibility to the convulsant pentylenetetrazol (PTZ). **A:** Dose-response curves for induction of clonic seizures demonstrate a greater PTZ sensitivity of *Cacna2d2*$^{-/-}$ mice compared to wild-type and heterozygous littermates. The curves show logistic fits to the data. The CD_{50} value obtained by the Spearman-Karber method for the null mutant is 26.6 mg/kg (95% confidence limit (CL): 21.4 to 33.1) compared with 52.0 mg/kg (95%CL: 47.7 to 56.8) and 55.8 mg/kg (95% CL: 49.23 to 63.2), respectively, for *Cacna2d2*$^{+/-}$ and *Cacna2d2*$^{+/+}$ animals. For each genotype, groups of three to six animals were tested at three to four doses. **B:** Seizure score values with increasing cumulative doses of PTZ. *Cacna2d2*$^{-/-}$ mice showed significantly greater behavioral seizure score values at the 10 and 20 mg/kg doses compared with *Cacna2d2*$^{+/+}$ and *Cacna2d2*$^{+/-}$ mice ($P < 0.008$, Kruskal-Wallis analysis of variance); eight animals were tested for each genotype. See "Experimental Procedures" for seizure score scale.

cerebellums isolated from *Cacna2d2*$^{-/-}$ and wild-type mice. Necropsy of mutant mice revealed no significant differences in the overall gross cerebellum anatomy or Purkinje cell layer architecture (Figure 7). Consistent lesions in the cerebellum, however, were detected in the granular layer. Apoptosis and thinning (loss of granule neurons) in the granule cell layers, especially in the vermis, was detected starting from day 22, becoming more profound later. Apoptosis in the granule cell layer was initially demonstrated with hematoxylin staining (Figure 8, A and B) and then verified with the TUNEL method and caspase-3 antibody (Figure 8, C and D, respectively). At P70 and later GFAP, immunoreactive glial cell processes became prominent in the granule cell layer (Figure 8, E and F). No apoptotic bodies were seen in *Cacna2d2*$^{+/+}$ or *Cacna2d2*$^{+/-}$ mice (data not shown). While no Purkinje

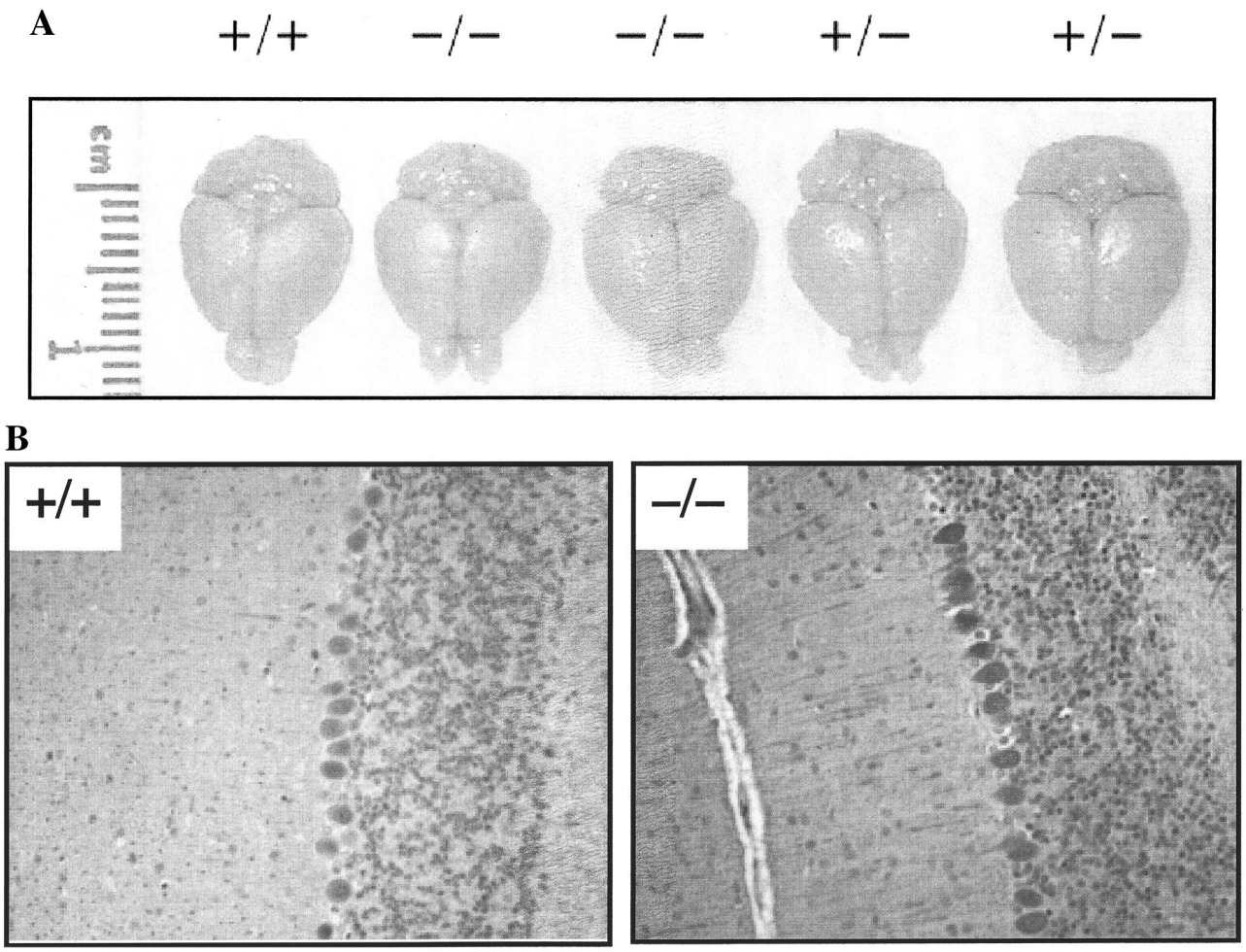

Figure 7. Cerebellar morphology of *Cacna2d2*^{tm1NCIF} mice. Cerebellums of young null mutants (P28-P38) are not different from their wt siblings by general appearance (**A**) or by Purkinje cells morphology as assessed by anti-calbindin staining (**B**, 16 cerebellar sections of each animal analyzed).

cells depletion was observed in *Cacna2d2*$^{-/-}$ mice at the age of about 1 month (Figure 7B), first signs of Purkinje cells depletion were noticed at P70 (Figure 8, A and B) and became more prominent later, especially in aging mice (> 1-year-old, data not shown). Since mice became clinically ill when these lesions appeared and were sacrificed or died soon thereafter, we could not determine the natural course of the lesions except in one 10-week-old mouse that exhibited reactive gliosis of Bergman glia in H&E stained sections. Lesions in other tissues, including severe thymic atrophy and suppurative rhinitis, were sometimes found in null mice. Pathological evaluation of *Cacna2d2*$^{-/-}$ hearts revealed no obvious abnormalities.

Discussion

Cerebellar Degeneration and Increased Seizure Susceptibility

The results of our study unequivocally implicate $\alpha 2\delta$-2 deficiency in cerebellar degeneration and ataxia, seizure susceptibility, and poor survival. Comparative analysis of this first $\alpha 2\delta$-type subunit knockout model, the spontaneous *ducky* mutant[23,24] that was recently shown to carry a *Cacna2d2* gene rearrangement,[25] and other previously characterized calcium neurological models facilitated identification of cells, currents, and mechanisms related to $\alpha 2\delta$-2 involvement in cerebellar ataxia. Homozygous inactivation of the *Cacna2d2* gene performed in this study produced a phenotype that had much in common with *ducky* and other epileptic models, such as *tottering*, *rolling Nagoya*, and *Cacna1a* ^{Fcrtm1}.[26–29] The observed similarities include ataxic gait, seizures, signs of cerebellar degeneration, and premature death.

Despite the fact that *Cacna2d2* normally shows broad expression in embryonic (Figure 4C) and adult[14] nervous tissue, neuronal degeneration observed in *Cacna2d2* null-mutants was restricted to the cerebellum. Limited impact of gene inactivation on the brain and other parts of nervous system may be explained by functional redundancy and overlapping tissue distribution reported for $\alpha 2\delta$ and $\alpha 1$ subunits.[8–10,14] The pathology observed in the cerebellar area included thinning of the granular layer in young mice followed by loss of Purkinje cells at older ages. Even though *Cacna2d2* expression was prominent

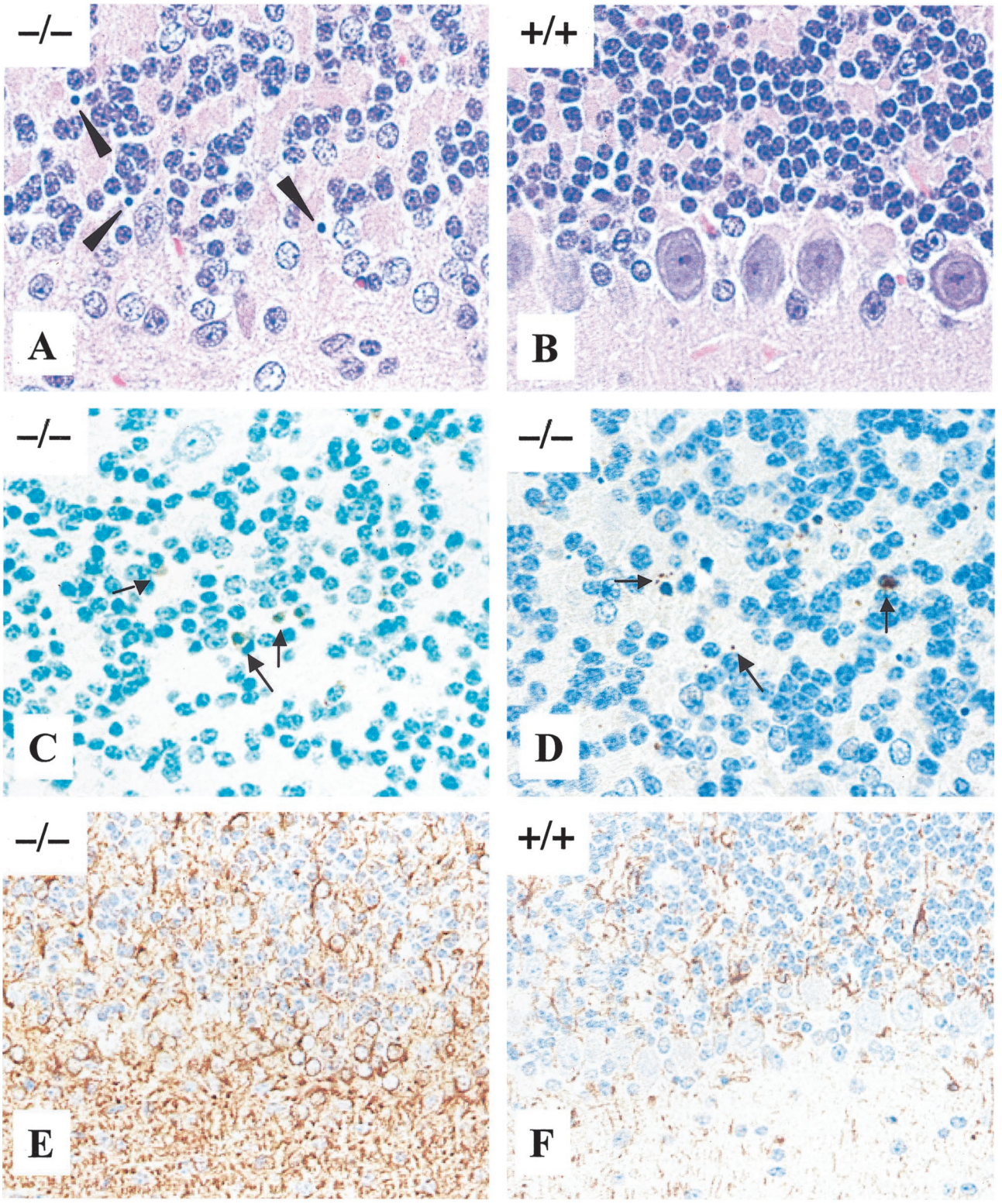

Figure 8. *Cacna2d2*$^{-/-}$ mice have reduced granule cell density and increased apoptosis in cerebellum. H&E-stained sections of cerebellum in null-mutant (**A**) and control (**B**) mice at P70 (magnification, ×90) show thinning of granule cell layer, deficiency of Purkinje cells, and presence of Bergmann's glia (reactive astrocytosis). **Arrowheads** in (**A**) indicate picnotic cells or apoptotic bodies. TUNEL (**C**) and caspase-3 antibody (**D**) staining show increased amount of apoptotic cells and bodies (**arrows**) in null mutant. Cerebellar cortex immunostaining with GFAP antibody (brown color) indicates enhanced expression of GFAP, representing glial cell proliferation (gliosis) in *Cacna2d2*$^{-/-}$ (**E**) in comparison with wild-type (**F**) (magnification, ×60).

Table 2. Comparison of *Cacna2d2* Mouse Models

Cacna2d2 mutant	Exons affected	Protein sequence affected	Reference
ducky	2-39 duplicated, 4-39 deleted	Loss of most of $\alpha 2$, the entire δ	25, 33
ducky^{2J}	9-39 (a 2-bp deletion in exon 9)	Loss of >800 C-terminal amino acids of $\alpha 2$, the entire δ	25, 33
Cacna2d2^{entla}	exon 3	Extra 39 amino acids, no disulfide linkage with δ	50
Cacna2d2^{tm1NCIF}	33-39 deleted	Loss of the 87 C-terminal amino acids of $\alpha 2$, the entire δ	This study

in the Purkinje layer and barely detectable in granular cells (Figure 4, A and B, and earlier observations [14]), the first sign of cerebellar degeneration in *Cacna2d2* null mice was the depletion of the granule cell layer (P22) via caspase 3-dependent apoptosis (Figure 8). Only later was this process followed by gradual loss of Purkinje cells, with most of them gone by 52 weeks (data not shown). This observation is consistent with the view that granular cells' survival during normal cerebellum development is largely dependent on forming proper connections with Purkinje cells[30] and that perturbations in Purkinje cells during critical stages of cerebellar development often result in devastating effects on granule cells.[31] Purkinje cell-dependent depletion of granular neurons was described also in another cerebellar neurodegenerative model, *lurcher* heterozygous mice.[32] Remarkably, *ducky* mice showed a quite distinct pattern of cerebellar pathology that included reduction in the gross size and appearance of cerebellum, demyelination, and early abnormalities in Purkinje cells morphology.[23–25,33] More severe cerebellar degeneration in *ducky* mutants may be associated with elimination of longer portions of the $\alpha 2\delta$-2 protein (Table 2) that may produce more acute effect on assembling, stability, and function of the entire multiprotein channel complex. Unfortunately, different genetic backgrounds of these two mutations (*du* on TKDU and *du*^{2J} on C57BLKS/J) complicates direct comparison of the *ducky* phenotypes with *Cacna2d2*$^{-/-}$ (129/SvJ:C57BL/6J background). Nevertheless, the work on *du* and *du*^{2J} [25,33] in conjunction with the present model provide strong evidence for a role of $\alpha 2\delta$-2 in promoting cerebellar neurons survival and functional interaction between granular and Purkinje neurons.

Concurrent with the histopathological signs of cerebellar degeneration, null mice developed multiple signs of neurological dysfunction, such as ataxia, clenching reflex, and dystonia, The fact that *Cacna2d2* null mice have normal serum somatotropic axis hormones (data not shown) implies that the observed growth delay is, most likely, a consequence of ataxia-associated indolent feeding behavior that causes fat depletion, dehydration, and malnutrition.

Another important feature that relates *Cacna2d2*-deficient mice to *Cacna1a* mutants is seizure-like behavior.[25–29] Spontaneous behavioral seizures in our model prompted us to use the chemoconvulsant PTZ to quantitatively assess seizure susceptibility/vulnerability. The null-mutants showed a significantly reduced PTZ threshold, demonstrating their enhanced seizure susceptibility. Given the electro-physiological flexibility of $\alpha 2\delta$ regulatory subunits and insufficiency in their number as compared to VDCC core subunits (3 types versus 10), one may expect that each of three $\alpha 2\delta$ subunits may be found *in vivo* in more than one calcium channel type. In addition to its association with P/Q-type ($Ca_V2.1$) channels as discussed above, it appears that $\alpha 2\delta$-2 may be the regulatory subunit of T-type ($Ca_V3.1$) Ca^{2+} channels that underlie rhythmogenesis in some central nervous system neurons involved in epileptic activity.[8,9,14] However, a recent study on mice with a targeted disruption of the $Ca_V3.1$ core subunit gene *Cacna1g* showed normal susceptibility to seizures.[34] This observation does not directly support the association of $\alpha 2\delta$-2 with T-type channels *in vivo*. Further characterization of cortical calcium channels and networks with $\alpha 2\delta$-2 involvement is required to verify whether P/Q channels may be solely responsible for increased seizure susceptibility in our model.

Most channelopathies associated with seizures result from alterations in channel function that are expected to enhance neuronal excitability.[35] An exception to this seems to be Ca^{2+} P/Q channelopathies where the epileptic phenotype occurs with reduced excitatory channel function. Different mechanisms were proposed to explain how a reduction in pre-synaptic P/Q currents might underlie spontaneous spike-and-wave discharges.[36,37] Based on experiments on co-expression of $\alpha 2\delta$-2 with a variety of VDCC core subunits and recordings made on $\alpha 2\delta$-2-deficient Purkinje cells,[7,8,14,24] the lack of the $\alpha 2\delta$-2 auxiliary subunit in *Cacna2d2*$^{-/-}$ mice would be also expected to diminish the depolarizing current contributing to neurotransmitter release. While the net effect of this alteration is difficult to predict, the epileptic phenotype is consistent with other Ca^{2+} channelopathies where a reduced Ca^{2+} current caused by defects in Ca^{2+} channel proteins does exist.[38] In this context, it is interesting to note that the antiepileptic drug gabapentin binds specifically and with high affinity to $\alpha 2\delta$-1 and $\alpha 2\delta$-2 proteins.[39] While a role for this interaction in the anticonvulsant activity of gabapentin is yet to be definitively established,[40] it is nevertheless intriguing that $\alpha 2\delta$-2 does appear to regulate seizure susceptibility, at least in the mouse mutants, suggesting that the interaction could very well be of clinical relevance.

Overall, our data unambiguously show that *Cacna2d2*, which is widely expressed in CNS (cerebellum, cortex, thalamus, spinal cord, etc) and dorsal ganglia (Figure 4 and[14]), is indispensable for central nervous system function and postnatal development. Based on the similarity between *Cacna1a* and *Cacna2d2* null phenotypes and their co-expression in Purkinje cells, it may be assumed that products of these genes serve as components of the same calcium channel, ie, $Ca_V2.1$ (P/Q). Indeed, this conclusion is supported by the reduction in the Purkinje P-type currents reported in *ducky* homozygotes.[25]

Premature Death and Cardiac Function

Although the *Cacna2d2*$^{-/-}$ mice that died at early age were runty and not thriving, there were no apparent behavioral changes or lesions that would account for sudden death. Since cardiac arrest is one of the most plausible mechanisms of unexpected death at young ages and in epileptic patients,[41–43] we assessed possible involvement of the *Cacna2d2* product in cardiac function. Taking into consideration that $\alpha 2\delta$-2 may serve as a regulatory subunit of multiple VDCCs,[8–10] we first identified human heart areas and nervous tissue where $\alpha 2\delta$-2 is expressed. Localization of *Cacna2d2* transcripts in heart-innervating sympathetic ganglia (Figure 4A) complemented reports on $\alpha 2\delta$-2 expression in rat root ganglia[44] and suggested that $\alpha 2\delta$-2 may be involved in autonomic regulation of cardiac function. Indeed, examination of the baseline ECG from conscious *Cacna2d2* null mice revealed a tendency to bradycardia (Table 1). Isoflurane anesthesia further unveiled abnormalities in null-mutants' heart rate regulation, suggesting that $\alpha 2\delta$-2 deficiency compromises response to the anesthetic. Volatile anesthesia produces its effect in the mammalian cerebral cortex by reduction in excitatory synaptic transmission, which, in turn, is caused by a decreased amount of transmitter glutamate in the synaptic cleft.[45] The observed difference in heart rate modulation, therefore, may be connected with the inability of *Cacna2d2* null-mutants to efficiently down-regulate synaptic calcium currents and the neurotransmitter release.

In summary, while our animal model provides, for the first time, evidence on $\alpha 2\delta$-2 involvement in cardiac rhythm regulation, no obvious cardiac mechanism was detected to explain the propensity to sudden death in the null mice. Recently, using ribonuclease protection assay Chu and Best[46] identified all three $\alpha 2\delta$ subunits' transcripts in rat heart atria. More studies into the structure and function of cardiac calcium channels are required to understand the exact roles of $\alpha 2\delta$-1, $\alpha 2\delta$-2, or $\alpha 2\delta$-3 in heart and the extent of their functional redundancy. Creating double $\alpha 2\delta$ mutants may help in answering this question and further assess the significance of $\alpha 2\delta$ subunits for cardiac function.

Clinical Significance of the Cacna2d2^{tm1NCIF} Model

In line with previously characterized *Cacna2d2 ducky* mutants, our model clearly implies a link between $\alpha 2\delta$-2 and congenital neurological disorders. Mutations in the *CACNA1A* gene encoding the core α1A subunit of the P/Q type VDCC have been associated in humans with familial hemiplegic migraine, episodic ataxia type-2, autosomal dominant spinocerebellar ataxia (SCA6), and idiopathic generalized epilepsies.[47–49] It is of utmost importance, therefore, to see if mutations in the human *CACNA2D2* gene from the 3p21.3 chromosomal region can produce effects similar to those observed in our animal model. The *Cacna2d2^{tm1NCIF}* model may also serve as a valuable tool for in-depth study of calcium-dependent neuronal death and development of therapies for P-type-channels-associated congenital disorders.

Note added in proof

While this manuscript was in review, a novel spontaneous *Cacna2d2* mutant, *Cacna2d2^{entla}*, was characterized and crossed into a C57BL/6J background.[50] This mutation produced an in-frame full-length $\alpha 2\delta$-2 protein with a 39 amino acids duplication in exon 3. The subunit was capable of incorporation into cellular membrane but failed to undergo proper processing to covalently bind the δ subunit. *Cacna2d2^{entla}* homozygotes showed a neurological phenotype and cerebellar morphology similar to our model.

Acknowledgments

We thank Drs. Alan Koretsky, Brenda Klaunberg, and Yukitaka Shizukuda for their support with animal ultrasound and ECG study, Eileen Southon and Susan Reid for help with generation of mouse lines, Dr. Eric Lander for providing the *Cacna2d2*-containing BAC clone, and Keith Rogers and Barbara Kasprzak for help with histological evaluation and immunohistochemistry.

References

1. Berridge MJ, Bootman MD, Lipp P: Calcium: a life and death signal. Nature 1998, 395:645–648
2. Santella L, Carafoli E: Calcium signaling in the cell nucleus. EMBO J 1997, 11:1091–1109
3. Catterall WA: Structure and regulation of voltage-gated Ca^{2+} channels. Annu Rev Cell Dev Biol 2000, 16:521–555
4. Randall A, Benham CD: Recent advances in the molecular understanding of voltage-gated Ca2+ channels. Mol Cell Neurosci 1999, 14:255–272
5. De Waard M, Gurnett CA, Campbell KP: Structural and functional diversity of voltage-activated calcium channels. Ion Channels 1996, 4:41–87
6. Hofmann F, Biel M, Flockerzi V: Molecular basis for Ca^{2+} channel diversity. Annu Rev Neurosci 1994, 17:399–418
7. Walker D, De Waard M: Subunit interaction sites in voltage-dependent Ca^{2+} channels: role in channel function. Trends Neurosci 1998, 21:148–154
8. Klugbauer N, Lacinova L, Marais E, Hobom M, Hofmann F: Molecular diversity of the calcium channel $\alpha 2\delta$ subunit. J Neurosci 1999, 19: 684–691
9. Gao B, Sekido Y, Maximov A, Saad M, Forgacs E, Latif F, Wei MH, Lerman M, Lee JH, Perez-Reyes E, Bezprozvanny I, Minna JD: Functional properties of a new voltage-dependent calcium channel $\alpha(2)\delta$ auxiliary subunit gene (CACNA2D2). J Biol Chem 2000, 275:12237–12242
10. Gong HC, Hang J, Kohler W, Li L, Su TZ: Tissue-specific expression and gabapentin-binding properties of calcium channel $\alpha 2\delta$ subunit subtypes. J Membr Biol 2001, 184:35–43
11. De Jongh KS, Warner C, Catterall WA: Subunits of purified calcium channels: α 2 and δ are encoded by the same gene. J Biol Chem 1990, 265:14738–14741
12. Lerman MI, Minna JD: The 630-kb lung cancer homozygous deletion region on human chromosome 3p21.3: identification and evaluation of the resident candidate tumor suppressor genes. Cancer Res 2000, 60:6116–6133
13. Gurnett CA, De Waard M, Campbell KP: Dual function of the voltage-dependent Ca^{2+} channel α 2 δ subunit in current stimulation and subunit interaction. Neuron 1996, 16:431–440

14. Hobom M, Dai S, Marais E, Lacinova L, Hofmann F, Klugbauer N: Neuronal distribution and functional characterization of the calcium channel $\alpha 2\delta$-2 subunit. Eur J Neurosci 2000, 12:1217–1226
15. Bonin A, Reid SW, Tessarollo L: Isolation, microinjection, and transfer of mouse blastocysts. Methods Mol Biol 2001, 158:121–134
16. Tessarollo L: Manipulating mouse embryonic stem cells. Methods Mol Biol 2001, 158:47–63
17. Shelton JM, Lee MH, Richardson JA, Patel SB: Microsomal triglyceride transfer protein expression during mouse development. J Lipid Res 2000, 41:532–537
18. Coughenour LL, Mclean JR, Parker RB: A new device for the rapid measurement of impaired motor function in mice. Pharmacol Biochem Behav 1977, 6:351–353
19. Crawley JN (editor): What's Wrong with My Mouse? New York, Wiley-Liss, 1999, pp 56–57
20. Schiller NB, Shah PM, Crawford M, DeMaria A, Devereux R, Feigenbaum H, Gutgesell H, Reichek N, Sahn E, Schnittger I: Recommendations for quantitation of the left ventricle by two-dimensional echocardiography. J Am Soc Echocardiogr 1989, 2:358–367
21. Devereux RB, Alonso DR, Lutas EM, Gottlieb GJ, Campo E, Sachs I, Reichek N: Echocardiographic assessment of left ventricular hypertrophy: comparison to necropsy findings. Am J Cardiol 1986, 57:450–458
22. Chu V, Otero JM, Lopez O, Sullivan MF, Morgan JP, Amende I, Hampton TG: Electrocardiographic findings in mdx mice: a cardiac phenotype of Duchenne muscular dystrophy. Muscle Nerve 2002, 26:513–519
23. Meier H: The neuropathology of ducky, a neurological mutation of the mouse: a pathological and preliminary histochemical study. Acta Neuropathol (Berl) 1968, 11:15–28
24. Burgess DL, Noebels JL: Single gene defects in mice: the role of voltage-dependent calcium channels in absence models. Epilepsy Res 1999, 36:111–122
25. Barclay J, Balaguero N, Mione M, Ackerman SL, Letts VA, Brodbeck J, Canti C, Meir A, Page KM, Kusumi K, Perez-Reyes E, Lander ES, Frankel WN, Gardiner RM, Dolphin AC, Rees M: Ducky mouse phenotype of epilepsy and ataxia is associated with mutations in the Cacna2d2 gene and decreased calcium channel current in cerebellar Purkinje cells. J Neurosci 2001, 21:6095–6104
26. Noebels JL, Sidman RL: Inherited epilepsy: spike-wave and focal motor seizures in the mutant mouse tottering. Science 1979, 204: 1334–1336
27. Fletcher CF, Lutz CM, O'Sullivan TN, Shaughnessy JD Jr, Hawkes R, Frankel WN, Copeland NG, and Jenkins NA: Absence epilepsy in tottering mutant mice is associated with calcium channel defects. Cell 1996, 87:607–617
28. Mori Y, Wakamori M, Oda S, Fletcher CF, Sekiguchi N, Mori E, Copeland NG, Jenkin NA, Matsushita K, Matsuyama Z, Imoto K: Reduced voltage sensitivity of activation of P/Q-type Ca^{2+} channels is associated with the ataxic mouse mutation rolling Nagoya (tg(rol)). J Neurosci 2000, 20:5654–5662
29. Fletcher CF, Tottene A, Lennon VA, Wilson SM, Dubel SJ, Paylor R, Hosford DA, Tessarollo L, McEnery MW, Pietrobon D, Copeland NG, Jenkins NA: Dystonia and cerebellar atrophy in Cacna1a null mice lacking P/Q calcium channel activity. EMBO J 2001, 15:1288–1290
30. Lossi L, Mioletti S, Merighi A: Synapse-independent and synapse-dependent apoptosis of cerebellar granule cells in postnatal rabbits occur at two subsequent but partly overlapping developmental stages. Neuroscience 2002, 112:509–523
31. Goldowitz D, Hamre K: The cells and molecules that make a cerebellum. Trends Neurosci 1998, 21:375–382
32. Wetts R, Herrup K: Interaction of granule, Purkinje, and inferior olivary neurons in lurcher chimeric mice: II. Granule cell death Neuroscience 2002, 112:509–523
33. Brodbeck J, Davies A, Courtney JM, Meir A, Balaguero N, Canti C, Moss FJ, Page KM, Pratt WS, Hunt SP, Barclay J, Rees M, Dolphin AC: The ducky mutation in Cacna2d2 results in altered Purkinje cell morphology and is associated with the expression of a truncated α 2 δ-2 protein with abnormal function. J Biol Chem 2002, 277:7684–7693
34. Kim D, Song I, Keum S, Lee T, Jeong M-J, Kim S-S, McEnery MW, Shin H-S: Lack of the burst firing of thalamocortical relay neurons and resistance to absence seizures in mice lacking α(1G) T-type Ca(2+) channels. Neuron 2001, 31:35–45
35. Rogawski MA: KCNQ2/KCNQ3 K^+ channels and the molecular pathogenesis of epilepsy: implications for therapy. Trends Neurosci 2000, 23:393–398
36. Caddick SJ, Wang C, Fletcher CF, Jenkins NA, Copeland NG, Hosford DA: Excitatory but not inhibitory synaptic transmission is reduced in lethargic (Cacnb4(lh)) and tottering (Cacna1atg) mouse thalami. J Neurophysiol 1999, 81:2066–2074
37. Zhang Y, Mori M, Burgess DL, Noebels JL: Mutations in high-voltage-activated calcium channel genes stimulate low-voltage-activated currents in mouse thalamic relay neurons. J Neurosci 2002, 22:6362–6371
38. Qian J, Noebels JL: Presynaptic Ca(2+) influx at a mouse central synapse with Ca(2+) channel subunit mutations. J Neurosci 2000, 20:163–170
39. Marais E, Klugbauer N, Hofmann F: Calcium channel α(2)δ subunits-structure and gabapentin binding. Mol Pharmacol 2001, 59:1243–1248
40. Rogawski MA: Principles of antiepileptic drug action. Antiepileptic Drugs, ed 5. Edited by Levy R, Mattson RH, Meldrum BS, Perucca E. Philadelphia, Lippincott Williams & Wilkins, 2002, pp 3–22
41. Fananapazir L, Epstein SE: Hemodynamic and electrophysiologic evaluation of patients with hypertrophic cardiomyopathy surviving cardiac arrest. Am J Cardiol 1991, 67:280–287
42. Atiga WL, Fananapazir L, McAreavey D, Calkins H, Berger RD: Temporal repolarization lability in hypertrophic cardiomyopathy caused by β-myosin heavy-chain gene mutations. Circulation 2000, 101: 1237–1242
43. Breningstall GN: Mortality in pediatric epilepsy. Pediatr Neurol 2001, 25:9–16
44. Yusaf SP, Goodman J, Pinnock RD, Dixon AK, Lee K: Expression of voltage-gated calcium channel subunits in rat dorsal root ganglion neurons. Neurosci Lett 2001, 28:137–141
45. Study RE: Isoflurane inhibits multiple voltage-gated calcium currents in hippocampal pyramidal neurons. Anesthesiology 1994, 81:104–116
46. Chu P-J, Best PM: Molecular cloning of calcium channel $\alpha 2\delta$-subunits from rat atria and the differential regulation of their expression by IGF-1. J Mol Cell Cardiol 2003, 35:207–215
47. Ophoff RA, Terwindt GM, Vergouwe MN, van Eijk R, Oefner PJ, Hoffman SM, Lamerdin JE, Mohrenweiser HW, Bulman DE, Ferrari M, Haan J, Lindhout D, van Ommen GJ, Hofker MH, Ferrari MD, Frants RR: Familial hemiplegic migraine and episodic ataxia type-2 are caused by mutations in the Ca^{2+} channel gene CACNL1A4. Cell 1996, 87:543–552
48. Hirose H, Arayama T, Takita J, Igarashi T, Hayashi Y, Nagao Y: A family of episodic ataxia type 2: no evidence of genetic linkage to the CACNA1A gene. Int J Mol Med 2003, 11:187–189
49. Zhuchenko O, Bailey J, Bonnen P, Ashizawa T, Stockton DW, Amos C, Dobyns WB, Subramony SH, Zoghbi HY, Lee CC: Autosomal dominant cerebellar ataxia (SCA6) associated with small polyglutamine expansions in the α 1A-voltage-dependent calcium channel. Nat Genet 1997, 15:62–69
50. Brill J, Klocke R, Paul D, Boison D, Gouder N, Klugbauer N, Hofmann F, Becker CM, Becker K: entla, a novel epileptic and ataxic Cacna2d2 mutant of the mouse. J Biol Chem 2004, 279:7322–7330